

## RESEARCH ARTICLES

## PALEOECOLOGY

# Abrupt warming events drove Late Pleistocene Holarctic megafaunal turnover

Alan Cooper,<sup>1,\*</sup> Chris Turney,<sup>2,\*</sup> Konrad A. Hughen,<sup>3</sup> Barry W. Brook,<sup>4,5</sup> H. Gregory McDonald,<sup>6</sup> Corey J. A. Bradshaw<sup>4</sup>

The mechanisms of Late Pleistocene megafauna extinctions remain fiercely contested, with human impact or climate change cited as principal drivers. We compared ancient DNA and radiocarbon data from 31 detailed time series of regional megafaunal extinctions and replacements over the past 56,000 years with standard and new combined records of Northern Hemisphere climate in the Late Pleistocene. Unexpectedly, rapid climate changes associated with interstadial warming events are strongly associated with the regional replacement or extinction of major genetic clades or species of megafauna. The presence of many cryptic biotic transitions before the Pleistocene/Holocene boundary revealed by ancient DNA confirms the importance of climate change in megafaunal population extinctions and suggests that metapopulation structures necessary to survive such repeated and rapid climatic shifts were susceptible to human impacts.

**T**he debate surrounding the causes of the extinctions of megafaunal species (terrestrial taxa with adults >45 kg), which occurred during the last glacial period (~110,000 to 11,650 calendar years ago; 110 to 11.65 ka) in the Late Pleistocene, has continued for over two centuries, since Cuvier first identified the mammoth and giant ground sloth (1–5). Although human activity as a result of hunting (“overkill”) and/or habitat modification and fragmentation are often cited as the principal driving force (1, 6–8), the diversity of extinction patterns observed on different continents has led to increasing recognition of the potential synergistic role of climate change (1–4, 9). A major confounding factor in the debate has been the coincident Late Pleistocene increase in human population size and dispersal into previously uninhabited areas, such as the New World, potentially exacerbating other ecological impacts.

Traditionally, a key argument against the potential role of climate-change impacts has been the paucity of identified extinction events during either previous glacial cycles or the many well-defined, climatic shifts recorded during the last glacial period (3, 4), including the Last Glacial

Maximum (LGM; ~23 to 19 ka) (Fig. 1). However, the lack of suitably resolved records of climate change and radiocarbon calibration on a common time scale makes such interpretations particularly challenging. The debate has also been constrained by the heavy reliance on fossil morphological evidence, precluding the identification of major genetic transitions or population-level turnovers. Recent work using ancient DNA (aDNA) has shown that morphological analyses of the Pleistocene paleontological record can have limited power to resolve species-level mammalian taxonomy issues or detect broad-scale genetic transitions at the population level, even when species suffer major genetic losses or almost go extinct (10–15). Indeed, aDNA and genomic studies have revealed a far more dynamic picture of megafaunal population ecology, including repeated localized extinctions, migrations, and replacements (10, 12–15).

The Late Pleistocene was characterized by a series of severe and rapid climate oscillations (regional temperature changes of up to 16°C) known as Dansgaard-Oeschger (D-O) interstadial (warming) events that have been identified in oceanic, ice, and terrestrial records throughout the Northern Hemisphere (16) (Fig. 1 and fig. S3). The millennial-length D-O events can be bundled into semi-regular cooling cycles with an asymmetrical saw-tooth pattern (Bond cycles) (17) that culminate in massive discharges of ice into the North Atlantic, known as Heinrich events. However, the precise timing, magnitude, and global extent of these events remain sufficiently uncertain to impair research into the effects of such rapid and extreme climate shifts on landscape and paleoecological change. In particular, there has been limited analysis of the potential relationship between rapid climate

change and major genetic transitions in widespread populations, marked by local extirpations or global extinctions of species and genetic diversity.

## Megafaunal data

To investigate this, we examined all available megafaunal species with comprehensive radiocarbon-dated series and plotted 31 calibrated major megafaunal transition events (defined as geographically widespread or global extinctions, or invasions, of species or major clades) that have been detected in either genetic (13 events) or paleontological (18 events) studies against the Greenland ice core record [on the Greenland Ice Core Chronology 2005 (GICC05) time scale] (18–20) (Fig. 1).

The genetic and radiocarbon data reveal a temporally staggered, long-term dynamic record of major megafaunal transitions across species with diverse ecologies and life histories. The events were widely distributed geographically across both Eurasia and the New World and included periods before human invasion. Multiple events appear to involve the rapid replacement of one species or population by a conspecific or congeneric across a broad area, often making the events undetectable in the fossil record on the basis of morphology, and potentially even in low-resolution genetic reconstructions of population paleodemography (21). These rapid replacements suggest that putative taphonomic biases (e.g., increased fossilization rates during either interstadials or stadials—cold periods) are not responsible for the apparent sudden disappearance or appearance of genetic diversity. Furthermore, common megafaunal fossils, such as mammoth, appear throughout the time period examined (Fig. 1). The apparent absence of extinctions during the cold conditions of the LGM, when Northern Hemisphere ice sheets reached their maximum volume, or to a lesser extent during the Younger Dryas stadial (11.7 to 12.7 kya; table S3) at the very end of the Pleistocene, is surprising, given that these events are commonly postulated as potential causes of megafaunal extinctions (3, 22). Although paleontological studies record range contractions into glacial refugia for many species during this period (4), it appears that, in general, cold conditions were not an important driver for extinctions, even in the presence of anatomically modern humans in Europe.

The megafaunal transitions appear to be centered around D-O warming events leading up to and then after the LGM, including a marked cluster of events around interstadials 5 to 7 in northern Europe (~37 to 32 ka; Fig. 1). A further well-known cluster of extinction events occurs during the termination of the Pleistocene (~14 to 11 ka), which has often been linked to the initial entry of humans into the New World (~15 ka) (6–8). However, half of the 12 extinction events in this period occur in western Eurasia, where modern humans arrived at least ~44 kya. Indeed, several taxa (e.g., mammoth) go extinct on the mainland of Eurasia considerably later than that of the New World, despite a much longer exposure to human hunting (3, 4) (Fig. 1).

<sup>1</sup>Australian Centre for Ancient DNA, School of Earth and Environmental Sciences, and Environment Institute, University of Adelaide, Adelaide, Australia. <sup>2</sup>Climate Change Research Centre and School of Biological, Earth, and Environmental Sciences, University of New South Wales, Sydney, Australia. <sup>3</sup>Woods Hole Oceanographic Institution, Woods Hole, MA 02543, USA. <sup>4</sup>Environment Institute and School of Biological Sciences, University of Adelaide, Adelaide, Australia. <sup>5</sup>School of Biological Sciences, University of Tasmania, Hobart, Australia. <sup>6</sup>Museum Management Program, National Parks Service, Fort Collins, CO 80525, USA.  
\*Corresponding author. E-mail: alan.cooper@adelaide.edu.au (A.C.); c.turney@unsw.edu.au (C.T.)

## Greenland-Cariaco climate time scale

A major challenge for testing whether the genetic transitions were synchronous with D-O events is the placement of megafaunal and climate records on a common time scale (23). Although the Greenland ice cores (18, 19) provide a detailed record of climate change for the North Atlantic, cumulative counting errors can exceed 2% (fig. S1) (20), resulting in calendar time scale offsets of up to 1000 years between Greenland D-O events and radiocarbon-calibrated megafaunal transitions (23, 24). To enable detailed comparisons, the climate and radiocarbon records should be on the same absolute time scale, which requires

the merging of different high-resolution data sets. Importantly, this also provides a means to improve the accuracy and the precision of the chronological framework and to assess the hemispheric nature of the climate shifts. One such approach is to use the abrupt shifts at the onset of D-O warming as tie points to correlate across multiple climate records (25), because these events caused widespread and rapid climate effects by decreasing the Northern Hemisphere temperature gradient (26), resulting in a poleward migration of the Intertropical Convergence Zone (ITCZ) and associated changes in tropical rainfall belts (27–31). In this regard, a key record is the Ven-

ezuelan Cariaco Basin marine sequence, which captures a climate record via shifts in the trade winds associated with northward migration of the ITCZ in the tropical Atlantic (20, 28), alongside a comprehensive suite of radiocarbon ages from planktonic foraminifera in the sediment core. The Cariaco sediments are annually laminated during the Late Glacial and Holocene, providing independent age control from 14.7 ka (32), before which distinct millennial-scale variability in sedimentological and geochemical proxies has been robustly correlated with the uranium series-dated Hulu Cave oxygen isotope ratio ( $\delta^{18}\text{O}$ ) speleothem record (with age uncertainties < 1%) (33).

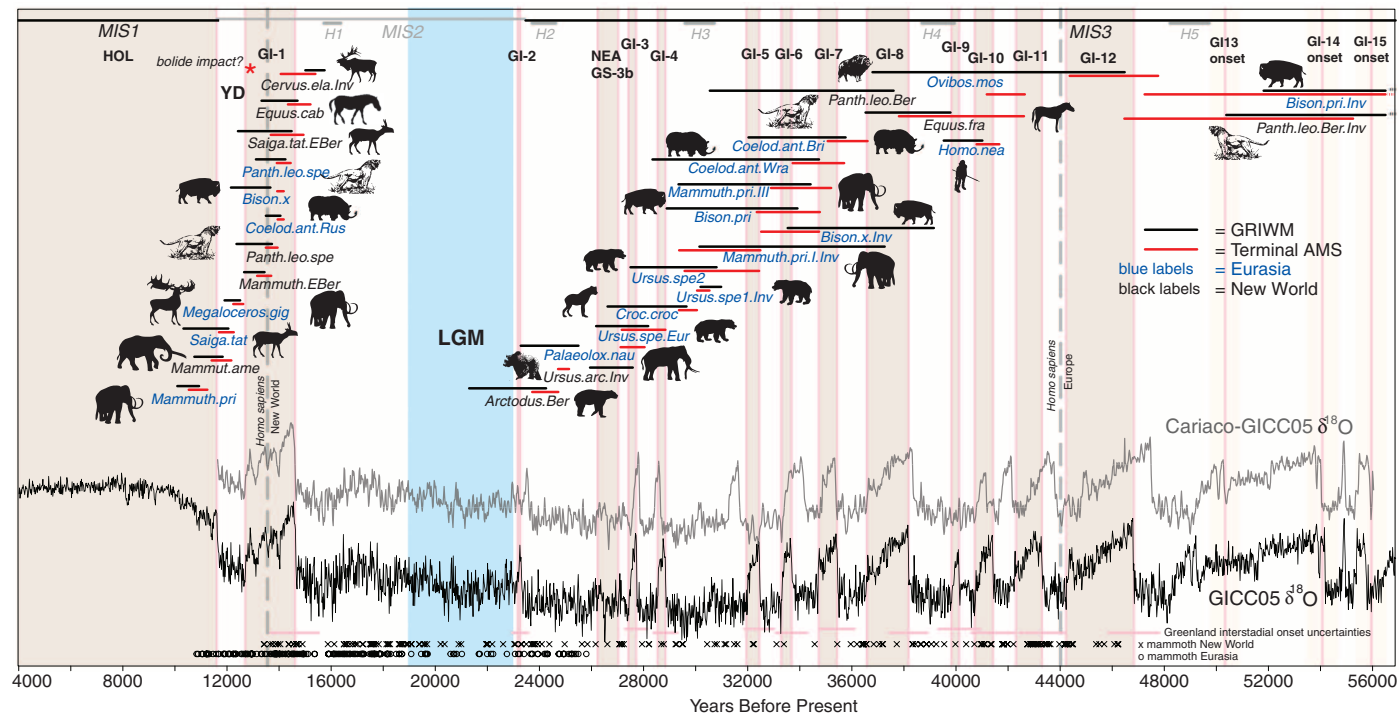


**Fig. 1. Megafaunal transition events and Late Pleistocene climate records.** Major megafaunal transition events (regionwide extinctions or global extinctions, or invasions, of species or major clades) identified in Late Pleistocene Holarctic megafaunal data sets through aDNA or paleontological studies, plotted on a reconstruction of Northern Hemisphere climate from the GICC05  $\delta^{18}\text{O}$  record (black wiggle curve). GICC05 interstadial warming events are shown with light gray boxes. There is an apparent absence of megafaunal events during the LGM (blue) and, to a lesser extent, the cold Younger Dryas stadial (YD) and a marked association with interstadials. Accelerator mass spectrometry (AMS) radiocarbon dates (red bar  $\pm 2$  SD, using Phase calibration in OxCal 4.1) calibrated by using the dendrodated IntCal <12,500-year data set (36) and Cariaco Basin (Hulu Cave) data set for older ages (28, 33), or GRIWM-based estimates of ghost ranges (black bar, 95% confidence interval) are given for each event (20). Eurasian taxa are shown in blue and New World in black, with animals facing right representing extinctions and those facing left representing invasions (.Inv.). The chronologically revised Greenland record, developed by combining the Cariaco Basin and Greenland ice core records, is also shown (dark gray wiggle curve) for the period >11.5 ka (because it is identical with GICC05 until this point) (20). Light pink bars (below) represent the error margins (1 SD) for the estimated onset of GI events in the published GICC05 chronology (19, 20). Heinrich events (Hx) are shown with marine isotope stages (MISx) in light gray at top (41). NEA-GS-3b was identified via Atlantic

marine sediment cores and radiocarbon dating (42). Calibrated radiocarbon ages (midpoints without laboratory dating errors) from mammoth remains in Eurasia (black circles) and New World (crosses) are plotted across the bottom of the figure to demonstrate the lack of obvious taphonomic hiatus during the time period analyzed (20). The approximate timing of the first presence of modern humans in North America (New World) and Europe are shown as vertical gray dashed lines. Abbreviated taxonomic names, with geographic area appended where necessary, are given: *Arctodus.Ber* (*Arctodus simus* East Beringia); *Bison.pri* (*Bison priscus* Europe); *Bison.x* (*Bison* n. sp. Europe); *Cervus.elia* (*Cervus elephas* New World); *Coelod.ant.Bri* (*Coelodonta antiquitatis* Britain); *Coelod.ant.Rus* (*C. antiquitatis* Russia); *Coelod.ant.Wra* (*C. antiquitatis* Wrangel Island); *Croc.croc* (*Crocuta crocuta spelaea* Europe); *Equus.cab* (*Equus caballus* East Beringia); *Equus.fra* (*E. francisci* East Beringia); *Homo.nea* (*Homo neanderthalensis* Europe); *Mammuth.pri* (*Mammuthus primigenius*); *Mammut.ame* (*Mammut americanum*); *Megaloceros.gig* (*Megaceros giganteus* Western Europe); *Ovibos.mos* (*Ovibos moschatus* Beringia); *Palaeolox.nau* (*Palaeoloxodon naumanni* Japan); *Panth.leo.Ber* (*Panthera leo spelaea* Beringia); *Panth.leo.spe* (*P. leo spelaea* Eurasia); *Saiga.tat* (*Saiga tatarica* Eurasia); *Ursus.arc* (*Ursus arctos* East Beringia); *Ursus.spe1* and *2* (*U. spelaea* Germany); *Ursus.spe.Eur* (*U. spelaea* Europe). [Further details of the geographic region and nature of each megafaunal event are presented in tables S1 and S2.]

We therefore used a D-O event tie-point approach to combine the calendar-age estimates obtained from Cariaco Basin (28) with the same interstadial events recorded in Greenland to allow a direct comparison between radiocarbon dates and climate change, thereby allowing us to test the apparent association between megafaunal extinction or replacement with warming events (Fig. 1). We find the timing of onsets of interstadial warming events in the two records to be statistically identical (20), allowing us to use OxCal 4.1 (34) to combine the two chronologies, and merged the calendar-dated onset of each interstadial in Cariaco with the annual layer-counted interstadial onset and duration from Greenland to generate a new combined record of the timing and duration of abrupt and extreme swings of north Atlantic temperature during the past 56 thousand years (Fig. 1 and tables S3 and S4) (20). Our new reconstruction shows that, although all current estimates of the onset of interstadial events in the GICC05  $\delta^{18}\text{O}$  record are within the errors of our combined Cariaco-Greenland chronology, the uncertainty surrounding these transitions is greatly reduced (by 18 to 79%) (Fig. 1, table S3, and figs. S2 and S4).

#### Testing climate-extinction associations

We used statistical resampling to test the distribution of megafaunal transitions for randomness relative to extreme and abrupt climatic events (either stadials or interstadials), using both the existing GICC05 and our new Cariaco-Greenland chronology (Fig. 1 and table S4) (20). We calculated the probability that the observed overlap between climate events and extinction or invasion events might be nonrandom by repeatedly randomizing the temporal position (but not duration) of the former and, for each iteration, counting the number of times overlap was observed with the latter. To do this, we used the calibrated radiocarbon age of the terminal observation of a clade or taxon (youngest age for extinctions, oldest for invasions) but also inferred unobserved temporal (ghost) ranges using the Gaussian-resampled, inverse-weighted McInerney (GRIWM) method (20, 35), which incorporates both sampling density and dating errors to estimate the most plausible temporal range of last or first occurrence. A nonrandom relationship was observed between interstadial events and megafaunal transitions for both the terminal observations and the GRIWM-based estimates, with statistical power depending on the number of transitions tested, but no such nonrandom overlap was detected for stadials (Fig. 2 and Table 1) (20). A nonrandom association is observed despite the uncertainties in the taphonomic, sampling, and dating processes involved in the data sets, and it is apparent with both the standard published GICC05 record and the new combined Cariaco-Greenland chronology (Table 1). A correlation can be seen even when terminal Pleistocene events are discarded to avoid the potential confounding impacts of human colonization (Fig. 2 and Table 1). The Younger Dryas stadial has also often been suggested as a prime climatic driver of extinctions

(3, 4, 22), but even for this event, the observed extinction events are distributed much more toward the preceding interstadial warm period (Fig. 1 and fig. S7), despite the larger dating uncertainties caused by radiocarbon plateaus at this time (36).

#### Interstadial impacts

The onsets of interstadials represent the most rapid and extreme changes observed in the Late Pleistocene climate record (Fig. 1) (20), and these are likely to have caused abrupt shifts in temperature or precipitation (either wetter or drier depending on local environments) away from a previous relatively stable state. These factors would have promoted changes in species ranges and distributions, potentially resulting in regional turnover. The local or regional expression of global climate variation (such as D-O events) is highly variable (37), and this is consistent with the megafaunal transition events being distributed broadly in terms of geography, taxonomy, and age.

This diffuse pattern, along with methodological limitations used in simple genetic paleodemographic reconstructions (27), might explain why correlations with climate events may have been difficult to detect previously. The lack of extinctions during the LGM is consistent with the stability of the climate during this period, albeit cold, in contrast with the large millennial-scale variability before and after, both of which coincide with high rates of extinctions.

The megafaunal taxa analyzed cover a wide range of life histories and ecological roles and include forest and steppe taxa. Many species have a broad niche (e.g., *Ursus arctos*, *Bison* spp., and Neandertals), making it difficult to classify taxa into cold- or warm-adapted groups as has previously been advocated (3, 4, 38). Furthermore, the rapid and drastic climate changes associated with both the onset and the end of interstadials, followed by new climate regimes, are potentially sufficient to disrupt populations of taxa across a

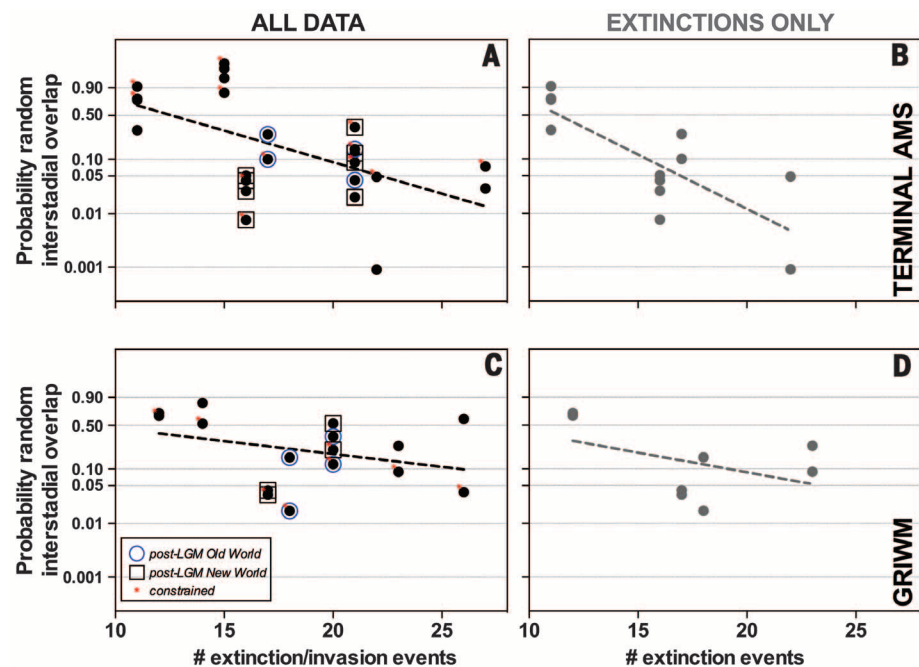


**Fig. 2. Randomization tests of the timing of megafaunal transitions with interstadial events.** Graphical representation of the simulation results presented in Table 1. The trend lines (dashed lines) show that the probability of generating the observed overlaps of megafaunal transition events with interstadials randomly ( $P$ ) is inversely related to the number of events examined, whereas, in contrast, the probabilities for stadials were all  $> 0.60$  (Table 1) (20). A strong correlation (steep gradient) was observed between megafaunal transitions (extinctions or invasion events) and interstadials using both: (A and B) terminal AMS  $^{14}\text{C}$  dates and (C and D) GRIWM estimates (which use a statistical model of extinction times based on a time series of records). The correlation was observed by using either the GICC05 (shown) or new combined Cariaco-Greenland (Table 1 and fig. S6) chronologies. The plotted data are from simulations excluding events with wide confidence intervals, because inclusion nearly always resulted in a greater chance of overlap being random [i.e., higher  $P$  values; see (20)]. To explore the effect of different combinations of megafaunal-transition events, we removed certain subsets and repeated the simulations: (i) excluding invasion events [(B) and (D)]—resulting in lower  $P$  of randomness; (ii) with a constrained-range overlap (red \*) applied to reduce error margins around an event where a rapid replacement by a congener or conspecific was observed (20)—producing little difference in the results; and (iii) with post-LGM events from either the New World (○) or Eurasia (□) only (to remove the potential effects of terminal Pleistocene human-associated impacts)—where low  $P$  were observed, but sample-size constraints limited the number of simulations able to detect nonrandom interstadial overlap (20). The results of these additional simulations are distributed along most of the power relationship, suggesting the correlations are not driven by any particular grouped subset of the data.

wide range of niches. The effects of high-amplitude climate change, followed by either stadial or interstadial conditions, are potentially compatible with previous suggestions that the extirpation of cold- or open-adapted taxa, such as woolly rhino and mammoth, occurred during interstadials and warm-adapted taxa, such as the giant deer, during stadials like the Younger Dryas (38). However, the widely dispersed temporal record of the megafaunal transitions suggests a markedly individualistic species response (39), presumably exaggerated by the localized environmental responses to climatic shifts (37). Simulations of paleovegetation patterns in the late Pleistocene have emphasized the importance of the duration and nature of inter-

stadial events and their impact on the growth of factors, such as forests (40). In contrast, we observe a more pronounced relationship between short interstadials (IS 3 to 7) and megafaunal events, rather than with the longer interstadials, such as 8 and 12, which might have been expected to allow larger-scale changes in the extent and nature of forest cover.

Our results lend strong empirical support to the hypothesis that environmental changes associated with rapid climatic shifts were important factors in the extinction of many megafaunal lineages. Indeed, the rapid replacement of local genetic populations by congeners or conspecifics (e.g., cave bears, bison, and mammoth) revealed

by aDNA suggests that broader-scale metapopulation structures or processes (e.g., long-distance dispersal, refugia, and rescue effects across spatially distributed subpopulations) were involved in maintaining ecosystem stability during the repeated phases of sudden climate change in the Pleistocene Holarctic. If so, human presence could have had a major and negative impact on megafaunal metapopulations by interrupting subpopulation connectivity, especially by concentrating on regular pathways between resource-rich zones (1), potentially leaving minimal signs of direct hunting. By interrupting metapopulation processes (e.g., dispersal and recolonization), humans could have both exacerbated regional extinctions brought

**Table 1. Randomization tests of the timing of megafaunal transitions with major climate events.**

Randomization tests of the timing of major megafaunal transitions with either interstadial or stadial events on the existing GICC05 and new combined Cariaco-Greenland time scales (20). The probabilities of generating the observed overlaps of extinction or invasion events at random with interstadials [P(rand) interstadials] and stadials [P(rand) stadials] are shown for both GRIWM and the phase-calibrated terminal AMS dates, along with probabilities expressed on the complementary log-log scale. The correlation tests revealed nonrandom overlap relationships between the number of events, *n*, and interstadials for both GICC05 and Cariaco-Greenland time scales. In contrast,

probabilities for overlaps at random with stadial events were >0.6 for both GRIWM and terminal AMS dates. Simulations producing low probabilities of generating the pattern of overlaps at random are cumulatively highlighted with asterisks ( $P < 0.1$ ), in blue ( $P < 0.05$ ), and in red ( $P < 0.01$ ). The power relationships for correlations with the GICC05 time scale are shown in Fig. 2. Simulations including terminal Pleistocene events from only the New World (NW) or Eurasia (Eur.) or neither (Pre-LGM) were used to explore the potentially confounding influences of human impact. Simulations using extinctions only (Extns) are indicated. The GICC05 time scale did not include interstadial NEA-GS-3b (table S3) because it is not detected in ice core records (41). CI, confidence interval.

Events (Eurasia, New World)	Extinctions / Invasions	Muskox	Wide-CI species	Constrained range overlaps	Number of events ( <i>n</i> )	Interstad GRIWM	Stadial GRIWM	Stadial AMS	Interstad P(random) Terminal AMS	Stadial P(random) Terminal AMS	Stadial P(random) Terminal AMS	Interstad P(random) Terminal AMS	Stadial P(random) Terminal AMS	Stadial P(random) Terminal AMS
All	All	✓	✓	✓	28	29	0.031*	0.228	0.801	0.999	0.126	0.220	0.998	0.998
All	All	✓	✓	x	28	29	0.109	0.009*	0.995	0.999	0.470	0.082*	0.989	0.999
All	All	x	✓	✓	27	28	0.024*	0.020*	0.974	0.997	0.066*	0.091*	0.983	0.996
All	All	x	x	✓	21	27	0.038*	0.075*	0.994	0.975	0.252	0.117	0.998	0.995
All	All	x	x	x	21	27	0.600	0.030*	0.992	0.999	0.487	0.037*	0.988	0.999
All	Extns	✓	✓	x	24	23	0.296	0.005*	0.999	0.992	0.396	0.023*	0.999	0.999
All	Extns	x	✓	x	22	22	0.097*	0.026*	0.994	0.974	0.302	0.031*	0.999	0.999
All	Extns	x	✓	✓	22	22	0.107	0.001*	0.965	0.999	0.023*	0.069*	0.999	0.997
All	Extns	x	x	✓	18	21	0.089*	0.048*	0.999	0.999	0.131	0.087*	0.994	0.999
All	Extns	x	x	x	18	21	0.249	0.001*	0.999	0.999	0.287	0.007*	0.999	0.999
Eur.	All	✓	✓	✓	22	24	0.018*	0.230	0.985	0.897	0.414	0.529	0.998	0.914
Eur.	All	✓	✓	x	23	24	0.453	0.046*	0.977	0.999	0.425	0.161	0.996	0.950
Eur.	All	x	✓	x	22	23	0.227	0.088*	0.962	0.822	0.250	0.164	0.994	0.980
Eur.	All	x	✓	✓	22	23	0.040*	0.105	0.958	0.864	0.019*	0.245	0.982	0.958
Eur.	All	x	x	✓	16	22	0.122	0.150	0.997	0.855	0.125	0.324	0.981	0.971
Eur.	All	x	x	x	16	22	0.347	0.042*	0.996	0.958	0.137	0.022*	0.986	0.987
Eur.	Extns	x	✓	✓	17	17	0.283	0.160	0.999	0.964	0.252	0.116	0.998	0.977
Eur.	Extns	x	x	✓	13	16	0.017*	0.100*	0.985	0.991	0.073*	0.424	0.997	0.959
Eur.	Extns	x	x	x	13	16	0.159	0.265	0.999	0.987	0.221	0.044*	0.992	0.997
NW	All	✓	✓	x	23	25	0.335	0.060*	0.385	0.996	0.354	0.075*	0.975	0.830
NW	All	x	✓	x	23	24	0.377	0.014*	0.977	0.996	0.283	0.099*	0.621	0.840
NW	All	x	x	✓	16	27	0.215	0.088*	0.943	0.960	0.382	0.231	0.775	0.865
NW	All	x	x	x	16	27	0.528	0.128	0.919	0.608	0.347	0.055*	0.883	0.899
NW	Extns	x	x	✓	13	17	0.034*	0.041*	0.848	0.929	0.111	0.124	0.943	0.956
NW	Extns	x	x	x	13	17	0.041*	0.026*	0.636	0.967	0.094*	0.061*	0.986	0.952
Pre-LGM	All	✓	✓	x	18	20	0.432	0.993	0.987	0.977	0.958	0.942	0.990	0.682
Pre-LGM	All	x	✓	x	17	19	0.918	0.966	0.999	0.611	0.961	0.879	0.999	0.818
Pre-LGM	Extns	x	x	✓	8	12	0.648	0.763	0.918	0.790	0.641	0.902	0.964	0.679
Pre-LGM	Extns	x	x	x	8	12	0.688	0.743	0.999	0.641	0.999	0.944	0.999	0.842

on by climate changes and allowed them to coalesce, potentially leading to the eventual regime shifts and collapses observed in megafaunal ecosystems. The lack of evidence for larger-scale ecological regime shifts during earlier periods of the Glacial (i.e., >45 ka) when interstadial events were common, but modern humans were not, supports a synergistic role for humans in exacerbating the impacts of climate change and extinction in the terminal Pleistocene events.

## REFERENCES AND NOTES

1. G. Haynes, *Quat. Int.* **285**, 89–98 (2013).
2. R. D. Guthrie, *Nature* **441**, 207–209 (2006).
3. P. L. Koch, A. D. Barnosky, *Annu. Rev. Ecol. Evol. Syst.* **37**, 215–250 (2006).
4. A. J. Stuart, A. M. Lister, *Quat. Sci. Rev.* **51**, 1–17 (2012).
5. G. Cuvier, Notice sur le squelette d'une très grande espèce de quadrupède inconnue jusqu'à présent, trouvé au Paraguay, et déposé au cabinet d'histoire naturelle de Madrid. *Magasin encyclopédique*, ou *Journal des Sciences, des Lettres et des Arts*, vol. 1, pp. 303–310 and vol. 2, pp. 227–228 (1796).
6. P. S. Martin, in *Quaternary Extinctions: A Prehistoric Revolution*, P. S. Martin, R. D. Klein, Eds. (Univ. of Arizona Press, Tucson, AZ, 1984).
7. J. Diamond, *J. Archaeol. Sci.* **16**, 167–175 (1989).
8. J. Alroy, *Science* **292**, 1893–1896 (2001).
9. E. D. Lorenzen et al., *Nature* **479**, 359–364 (2011).
10. I. Barnes, P. Matheus, B. Shapiro, D. Jensen, A. Cooper, *Science* **295**, 2267–2270 (2002).
11. M. Bunce et al., *Nature* **425**, 172–175 (2003).
12. B. Shapiro et al., *Science* **306**, 1561–1565 (2004).
13. M. Hofreiter, J. Stewart, *Curr. Biol.* **19**, R584–R594 (2009).
14. W. Miller et al., *Proc. Natl. Acad. Sci. U.S.A.* **109**, E2382–E2390 (2012).
15. S. Brace et al., *Proc. Natl. Acad. Sci. U.S.A.* **109**, 20532–20536 (2012).
16. E. W. Wolff, J. Chappellaz, T. Blunier, S. O. Rasmussen, A. Svensson, *Quat. Sci. Rev.* **29**, 2828–2838 (2010).
17. G. Bond et al., *Nature* **365**, 143–147 (1993).
18. S. O. Rasmussen et al., *J. Geophys. Res.* **111**, D06102 (2006).
19. A. Svensson et al., *Clim. Past* **4**, 47–57 (2008).
20. See supplementary materials available on Science Online.
21. T. Mourier, S. Y. Ho, M. T. Gilbert, E. Willerslev, L. Orlando, *Mol. Biol. Evol.* **29**, 2241–2251 (2012).
22. G. M. MacDonald et al., *Nat. Commun.* **3**, 893 (2012).
23. R. Muscheler, F. Adolph, A. Svensson, *Earth Planet. Sci. Lett.* **394**, 209–215 (2014).
24. C. Buizert et al., *Clim. Past* **11**, 153–173 (2015).
25. N. J. Shackleton, R. G. Fairbanks, T. C. Chiu, F. Parrenin, *Quat. Sci. Rev.* **23**, 1513–1522 (2004).
26. J. T. Overpeck, L. C. Peterson, N. Kipp, J. Imbrie, D. Rind, *Nature* **338**, 553–557 (1989).
27. K. A. Hughen, J. T. Overpeck, L. C. Peterson, S. Trumbore, *Nature* **380**, 51–54 (1996).
28. K. Hughen, J. Suthon, S. Lehman, C. Bertrand, J. Turnbull, *Quat. Sci. Rev.* **25**, 3216–3227 (2006).
29. L. C. Peterson, G. H. Haug, K. A. Hughen, U. Röhl, *Science* **290**, 1947–1951 (2000).
30. S. C. Porter, A. Zhiseng, *Nature* **375**, 305–308 (1995).
31. Y. Wang et al., *Nature* **451**, 1090–1093 (2008).
32. K. A. Hughen, J. R. Suthon, C. J. H. Bertrand, B. Frantz, P. Zermeno, *Radiocarbon* **46**, 1161–1187 (2004).
33. T. J. Heaton, E. Bard, K. Hughen, *Radiocarbon* **55**, 1975–1997 (2013).
34. C. B. Ramsey, *Radiocarbon* **51**, 337–360 (2009).
35. C. J. A. Bradshaw, A. Cooper, C. S. M. Turney, B. W. Brook, *Quat. Sci. Rev.* **33**, 14–19 (2012).
36. P. J. Reimer et al., *Radiocarbon* **55**, 1869–1887 (2013).
37. X. A. S. Wang et al., *Geophys. Res. Lett.* **34**, L23701 (2007).
38. A. J. Stuart, P. A. Kosintsev, T. F. G. Higham, A. M. Lister, *Nature* **431**, 684–689 (2004).
39. J. R. Stewart, *J. Evol. Biol.* **22**, 2363–2375 (2009).
40. B. Huntley et al., *PLOS ONE* **8**, e61963 (2013).
41. P. C. Tzedakis, K. A. Hughen, I. Cacho, K. Harvati, *Nature* **449**, 206–208 (2007).
42. W. E. N. Austin et al., *Quat. Sci. Rev.* **36**, 154–163 (2012).

## ACKNOWLEDGMENTS

We thank the following museums and curators for their generous assistance with samples, advice and encouragement: Canadian Museum of Nature (R. Harington); American Museum of Natural History (R. Tedford); Natural History Museum London (A. Curran); Yukon Heritage Centre (J. Storer and G. Zazula); University of Alaska, Fairbanks (D. Guthrie, C. Gerlach, and P. Matheus), Royal Alberta Museum (J. Burns); Institute of Plant and Animal Ecology, RAS Yekaterinburg (P. Kosintsev and A. Vorobiev); Laboratory of Prehistory, St. Petersburg (V. Doronichev and L. Golovanova); D. Froese; T. Higham; A. Sher; J. Glimmerveen; B. Shapiro; T. Gilbert; E. Willerslev; R. Barnett; Yukon miners (B. and R. Johnson, the Christie family, K. Tatlow, S. and N. Schmidt); L. Dalen and J. Soubrier for data and assistance. This work was supported by NSF NESTC workshop "Integrating datasets to investigate megafaunal extinction in the late Quaternary." A.C., C.T., B.W.B., and C.J.A.B. were supported by Australian Research Council Federation, Laureate and Future Fellowships. The new GICC05-Cariaco Basin  $\delta^{18}\text{O}$  record is provided in (20) and also

lodged on the Paleoclimatology Database (National Oceanic and Atmospheric Administration dataset ID: noaa-icecore-19015). The previously published radiocarbon data, with original references, is presented in (20). A.C. and C.T. conceived and performed research; A.C., C.J.A.B., C.T., and B.W.B. designed methods and performed analysis; A.C. and C.T. wrote the paper with input from all authors.

## SUPPLEMENTARY MATERIALS

[www.sciencemag.org/content/349/6248/602/suppl/DC1](http://www.sciencemag.org/content/349/6248/602/suppl/DC1)  
Materials and Methods  
Supplementary Text  
Figs. S1 to S8  
Tables S1 to S4  
References (43–54)

27 April 2015; accepted 3 July 2015  
Published online 23 July 2015  
10.1126/science.aac4315

## IMMUNODEFICIENCIES

## Impairment of immunity to *Candida* and *Mycobacterium* in humans with bi-allelic *RORC* mutations

Satoshi Okada,<sup>1,2\*</sup> Janet G. Markle,<sup>1,\*†</sup> Elissa K. Deenick,<sup>3,4‡</sup> Federico Mele,<sup>5‡</sup> Dina Averbuch,<sup>6‡</sup> Macarena Lagos,<sup>7,8‡</sup> Mohammed Alzahrani,<sup>9‡</sup> Saleh Al-Muhsen,<sup>9,10‡</sup> Rabih Halwani,<sup>10</sup> Cindy S. Ma,<sup>3,4</sup> Natalie Wong,<sup>3</sup> Claire Soudais,<sup>11</sup> Lauren A. Henderson,<sup>12</sup> Hiyan Marzouqa,<sup>13</sup> Jamal Shamma,<sup>13</sup> Marcela Gonzalez,<sup>7</sup> Rubén Martínez-Barricarte,<sup>1</sup> Chizuru Okada,<sup>1</sup> Danielle T. Avery,<sup>3</sup> Daniela Latorre,<sup>5</sup> Caroline Deswarie,<sup>14,15</sup> Fabienne Jabot-Hanin,<sup>14,15</sup> Egidio Torrado,<sup>16§</sup> Jeffrey Fountain,<sup>16||</sup> Aziz Belkadi,<sup>14,15</sup> Yuval Itan,<sup>1</sup> Bertrand Boisson,<sup>1</sup> Mélanie Migaud,<sup>14,15</sup> Cecilia S. Lindestam Arlehamn,<sup>17</sup> Alessandro Sette,<sup>17</sup> Sylvain Breton,<sup>18</sup> James McCluskey,<sup>19</sup> Jamie Rossjohn,<sup>20,21,22</sup> Jean-Pierre de Villartay,<sup>23</sup> Despina Moshous,<sup>23,24</sup> Sophie Hambleton,<sup>25</sup> Sylvain Latour,<sup>26</sup> Peter D. Arkwright,<sup>27</sup> Capucine Picard,<sup>1,14,15,24,28</sup> Olivier Lantz,<sup>11</sup> Dan Engelhard,<sup>6</sup> Masao Kobayashi,<sup>2</sup> Laurent Abel,<sup>1,14,15</sup> Andrea M. Cooper,<sup>16||</sup> Luigi D. Notarangelo,<sup>12,29||</sup> Stéphanie Boisson-Dupuis,<sup>1,14,15¶</sup> Anne Puel,<sup>1,14,15¶</sup> Federica Sallusto,<sup>5,30#</sup> Jacinta Bustamante,<sup>1,14,15,28#</sup> Stuart G. Tangye,<sup>3,4#</sup> Jean-Laurent Casanova<sup>1,14,15,24,31+</sup>

Human inborn errors of immunity mediated by the cytokines interleukin-17A and interleukin-17F (IL-17A/F) underlie mucocutaneous candidiasis, whereas inborn errors of interferon- $\gamma$  (IFN- $\gamma$ ) immunity underlie mycobacterial disease. We report the discovery of bi-allelic *RORC* loss-of-function mutations in seven individuals from three kindreds of different ethnic origins with both candidiasis and mycobacteriosis. The lack of functional ROR $\gamma$  and ROR $\gamma$ T isoforms resulted in the absence of IL-17A/F-producing T cells in these individuals, probably accounting for their chronic candidiasis. Unexpectedly, leukocytes from ROR $\gamma$ - and ROR $\gamma$ T-deficient individuals also displayed an impaired IFN- $\gamma$  response to *Mycobacterium*. This principally reflected profoundly defective IFN- $\gamma$  production by circulating  $\gamma\delta$  T cells and CD4 $^+$ CCR6 $^+$ CXCR3 $^+$   $\alpha\beta$  T cells. In humans, both mucocutaneous immunity to *Candida* and systemic immunity to *Mycobacterium* require ROR $\gamma$ , ROR $\gamma$ T, or both.

Inborn errors of human interleukin-17A and interleukin-17F (IL-17A/F) or interferon- $\gamma$  (IFN- $\gamma$ ) immunity are each associated with a specific set of infections. Inborn errors of IL-17A/F underlie chronic mucocutaneous candidiasis (CMC), which is characterized by infections of the skin, nails, and oral and genital mucosae with *Candida albicans*, typically in the absence of other infections. Five genetic etiologies of CMC have been reported, with mutations in

five genes (1, 2). Inborn errors of IFN- $\gamma$  underlie Mendelian susceptibility to mycobacterial disease (MSMD), which is characterized by selective susceptibility to weakly pathogenic mycobacteria, such as *Mycobacterium bovis* Bacille Calmette-Guérin (BCG) vaccines and environmental mycobacteria. Eighteen genetic etiologies of MSMD have been reported, involving mutations of nine genes (3, 4). Only a few patients display both candidiasis and mycobacteriosis, including some

*This copy is for your personal, non-commercial use only.*

If you wish to distribute this article to others, you can order high-quality copies for your colleagues, clients, or customers by [clicking here](#).

Permission to republish or repurpose articles or portions of articles can be obtained by following the guidelines [here](#).

The following resources related to this article are available online at  
[www.sciencemag.org](http://www.sciencemag.org) (this information is current as of August 6, 2015):

Updated information and services, including high-resolution figures, can be found in the online version of this article at:

<http://www.sciencemag.org/content/349/6248/602.full.html>

Supporting Online Material can be found at:

<http://www.sciencemag.org/content/suppl/2015/07/22/science.aac4315.DC1.html>

A list of selected additional articles on the Science Web sites related to this article can be found at:

<http://www.sciencemag.org/content/349/6248/602.full.html#related>

This article cites 51 articles, 8 of which can be accessed free:

<http://www.sciencemag.org/content/349/6248/602.full.html#ref-list-1>

This article appears in the following subject collections:

Ecology

<http://www.sciencemag.org/cgi/collection/ecology>